Article ID:1004-4213(2010)08-1519-5

Comparison of Interface and Confined Phonons in Wurtzite Quantum Cascade Laser*

CHEN Gui-chu[1], FAN Guang-han[2]
(1 *Department of Physics, Zhaoqing University, Zhaoqing, Guangdong* 526061, *China*)
(2 *Institute of Optoelectronic Material and Technolochy, South China Normal University, Guangzhou* 510631, *China*)

Abstract: The interface and confined phonon modes of the wurtzite quantum cascade laser are investigated using the transfer-matrix method. One group of interface modes and two groups of confined modes are presented in the longitudinal optical frequency domain, and the interface modes can be transited into the confined modes for two lowest frequency modes. The dispersions and electronic potentials of the interface and confined modes are obviously different, and the scattering rate induced by the confined mode is comparable to that induced by the interface mode.

Key words: AlGaN/GaN, QCL, interface, confined, scattering rate
CLCN: O431.2 **Document Code**: A **doi**: 10.3788/gzxb20103908.1519

0 Introduction

The quantum cascade laser (QCL) is an important semiconductor laser source from the point of view of basic reseach and potential applications[1-3]. Its structure is composed of many periods, in which a special type of semiconductor heterostructrue is grown with some alternating layers of different materials and with varying thicknesses. Sun[4] and Huang[5] propose to use a GaN-based system with large LO-phonon energy (~90 meV) for THz QCLs aiming at achieving high temperature operation. The GaN-based material usually crystallize in the hexagonal wurtzite structure[6-7]. Every primitive cell in wurtzite contains four atoms, and nine optical and three acoustical branchs are presented. Only two optical phonon are both Raman and infrared active, which correspond to the A_1 and E_1 modes[8]. The A_1 and E_1 modes all split into longitudinal-optical (LO) and transverse-optical (TO) components.

Several theoretical investigation based on the DC model and London's uniaxial model have so far been presented to the polar optical phonons in wurtzite GaN-based heterojunctions[9-15]. Among them, Chen utilizes the macroscopic dielectric continuum (MDC) approach, and Lu utilizes the transfer-matrix method (TMM) to study the interface and confined phonons of GaN/ZnO quantum well. TMM is also adopted by Gleize to describe the interface and confined phonons of GaN quantum well and GaN/AlN superlattice. In this present paper, TMM is used to investigate the interface and confined phonons in AlGaN/GaN QCL. The valuable conclusions are achieved by comparing the phonon spectra, potentials, and electron-phonon interactions of the interface modes with those of the confined modes.

1 TMM theory model for QCL

The wurtzite $Al_{0.15}Ga_{0.85}N$/GaN three-well QCL proposed by Sun is considered here[4], and the width of each layer in one period is 3.0, 4.0, 3.0, 2.5, 2.0, 2.5 nm, respectively, where the boldface number is indicated as the width of wells. The electron energy levels and wavefunctions of subband in one period are shown in Fig. 1, which

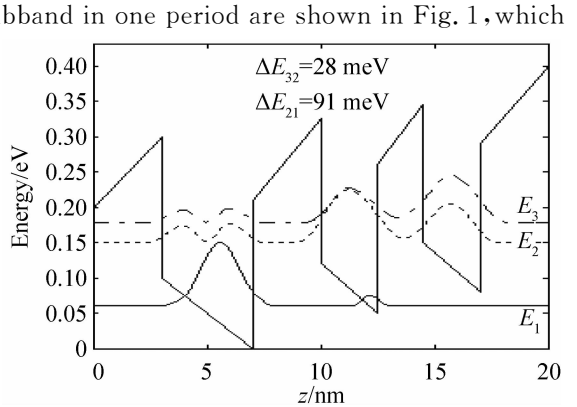

Fig. 1 Band structure, subband energy separations and wavefunctions of one period under the external bias $E=7.0\times10^4$ V/cm

*Supported by the National Natural Science Foundation of China (50602018) and the Important Item in Key Domain of Guangdong and Hongkong(2007A010501008)
Tel: 13760012915 Email: gchenbox@163.com
Received date: 2009-10-19 Revised date: 2010-03-12

can be calculated by solving the effective mass Schrodinger and Poisson′s equations self-consistently.

The phonon mode in each layer can be regarded as the linear combination of spatial functions and can be rewritten as[12]

$$\phi_j(z)=A_j e^{iq_j z}+B_j e^{-iq_j z} \tag{1}$$

where

$$q_j=\sqrt{-(\varepsilon_{j,\perp}/\varepsilon_{j,z})}q \tag{2}$$

the boundary conditions satisfy that the continuity of the tangential component of the electric field and the z component of the displacement vector must be continuous at the interfaces.

$$\varepsilon_{j,z}\frac{\partial\phi_j(z)}{\partial z}\bigg|_{z=z_j}=\varepsilon_{j+1,z}\frac{\partial\phi_{j+1}(z)}{\partial z}\bigg|_{z=z_j} \tag{3}$$

$$\phi_j(z)\big|_{z=z_j}=\phi_{j+1}(z)\big|_{z=z_j} \tag{4}$$

Applying the boundary conditions, we can obtain the TM related to the successive layers as follow

$$M_{j,j+1}=\frac{1}{2}\begin{Bmatrix}(1+\alpha_{j,j+1})e^{i(q_{j,z}-q_{j+1,z})z_j}\cdots\cdots(1-\alpha_{j,j+1})e^{-i(q_{j,z}+q_{j+1,z})z_j}\\(1-\alpha_{j,j+1})e^{i(q_{j,z}+q_{j+1,z})z_j}\cdots\cdots(1+\alpha_{j,j+1})e^{-i(q_{j,z}-q_{j+1,z})z_j}\end{Bmatrix} \tag{5}$$

where $\alpha_{j,j+1}=k_j,\varepsilon_{j,z}/(k_{j+1}\varepsilon_{j+1,z})$, and the total matrix between the first and the last layer is denoted as

$$M_{\mathrm{tot}}=\begin{pmatrix}M_{11}\cdots M_{12}\\M_{21}\cdots M_{22}\end{pmatrix}=\prod_{j=0}^{N}M_{i,j+1} \tag{6}$$

To suit the calculation of TMM, the width of the first barrier in Fig. 1 is changed from 3 nm to ∞. There will be six interfaces to be treated within the TMM theory. In addition, the attenuation condition requires that the phonon modes should be zero as z tends to $\pm\infty$, i. e. , $A_0=B_6=0$. Consequently we can obtain the phonon spectra from this formula, i. e. , $M_{22}=0$. Due to the anisotropy of wurtzite structure, the dielectric function is classified into two types

$$\varepsilon_\perp(\omega)=\varepsilon_\perp^{(\infty)}\frac{\omega^2-\omega_{\perp L}^2}{\omega^2-\omega_{\perp T}^2},\varepsilon_z(\omega)=\varepsilon_z^{(\infty)}\frac{\omega^2-\omega_{zL}^2}{\omega^2-\omega_{zT}^2} \tag{7}$$

where $\varepsilon_\perp^{(\infty)}$ and $\varepsilon_z^{(\infty)}$ are the optical dielectric constants, and the relation $\varepsilon_\perp^{(\infty)}=\varepsilon_z^{(\infty)}$ is satisfied with good accuracy[7], $\omega_{\perp L}$ and ω_{zL} are the zone center longitudinal E_1(LO) and A_1(LO) phonon frequencies, $\omega_{\perp T}$ and ω_{zT} are the zone center transverse E_1(TO) and A_1(TO) phonon frequencies. If $\varepsilon_\perp(\omega)\varepsilon_z(\omega)>0$, together with $\varepsilon_{j,z}(\omega)\varepsilon_{j+1,z}(\omega)<0$, is satisfied for each layer, we will obtain the interface phonon modes[7]. Otherwise, if $\varepsilon_\perp(\omega)\varepsilon_z(\omega)>0$ is satisfied for barrier layers and $\varepsilon_\perp(\omega)\varepsilon_z(\omega)<0$ is satisfied for well layers, the confined phonon modes will be achieved.

2 Interface and confined phonons in QCL

In our calculations, we take $d=14$ nm, and the material parameters, i. e. , the zone-center TO and LO frequencies of GaN and $Al_{0.15}Ga_{0.85}N$ are cited from Ref. [7]. Fig. 2 shows the dispersions of

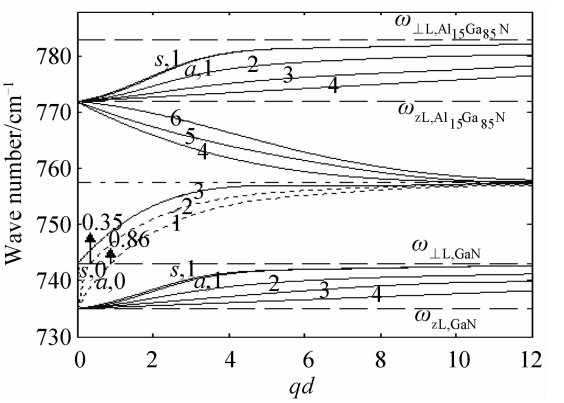

Fig. 2 The dispersion of interface and confined phonons in $Al_{0.15}Ga_{0.85}N$/GaN QCL

interface and confined phonons of wurtzite QCL. The characteristic phonon frequencies are shown by the dashed lines. The dot-dashed lines indicate the resonant frequency for IF mode. There are six interface modes, corresponding to $[\omega_{\perp L,\mathrm{GaN}},\omega_{zL,AlGaN}]$, and two groups of quantumized confined modes, corresponding to $[\omega_{zL,\mathrm{GaN}},\omega_{\perp L,\mathrm{GaN}}]$ (C_{I} domain) and $[\omega_{zL,\mathrm{AlGaN}},\omega_{\perp L,\mathrm{AlGaN}}]$ (C_{II} domain), respectively. An interesting consequence is presented that $q\neq0$ and $q_{\mathrm{GaN}}=0$ when the interface modes 1 and 2 (labeled from low to high frequency) approach $\omega_{\perp L}$ of GaN. We know the modes 1 and 2 will be changed into the confined modes $a,0$ and $s,0$ with purely real q_{GaN} in GaN well, if qd is less than the values denoted in Fig. 2. The confined modes are denoted with quantum number m and the quasi-symmetric property: symmetric (s) and antisymmetric (a). The reason for the prefix "quasi-" to be added is that the space is not strictly symmetric according to the middle plane of one period. The modes 0 and 1 in the C_{I} domain, and the mode 1 in the C_{II} domain, are nondegenerate, furthermore these modes approach

$\omega_{\perp L}$ of GaN and AlGaN, respectively, when $qd \to \infty$.

Based on the known dispersion relations, we can get the electrostatic potential distribution of the phonon modes. The normalization of the phonon potential can be obtained from the orthonormality and completeness conditions of the phonon eigenfunctions. For the wurtzite, the normalization condition is given by

$$\frac{\hbar}{2\omega}=\sum_i \frac{\varepsilon_0}{2\omega}\int_{\text{layer},j} dz\left[q_\perp \frac{\partial \varepsilon_{\perp,j}(\omega)}{\partial \omega}|p_\perp^{(j)}(q_\perp,z)|^2+\frac{\partial \varepsilon_{z,j}(\omega)}{\partial \omega}\left|\frac{\partial p_\perp^{(j)}(q_\perp,z)}{\partial z}\right|^2\right] \quad (8)$$

From this condition, the potentials of interface modes s, 2 and a, 5 are shown in Fig. 3. The decaying amplitude of mode a, 5 from the interfaces is far stronger than that of mode s, 2. Fig. 4 shows

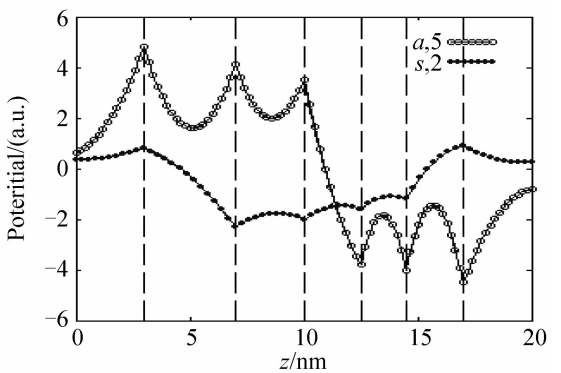

Fig. 3　The phonon potentials of modes s, 2 and a, 5 at $q=0.3$ nm^{-1}

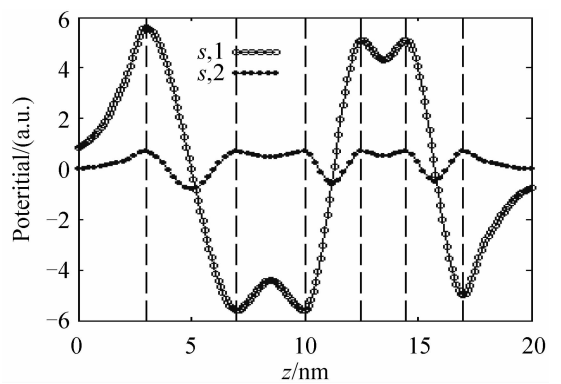

Fig. 4　The phonon potentials of modes s, 1 and s, 1 in C_I domain at $q=0.3$ nm^{-1}

the potentials of modes s, 1 and a, 1 in the C_I domain, and the amplitude of mode s, 1 is almost 10 times stronger than that of mode s, 2. We can see that the C_I modes are not strictly confined in the wells and they can penetrate into the barrier, so we call them quasi-confined modes. Fig. 5 shows the potentials of modes a, 1 and a, 1 in the C_{II} domain, and all the C_{II} modes are strictly confined in the wells, as is the same as the confined phonons in the cubic heterostructure. Since the amplitude of the confined modes largely decreases with the increasing qantum number m, it is safe to include only the first three modes, i. e., $m=0, 1, 2$ for the C_I modes and $m=1, 2, 3$ for the C_{II} modes in calculating the electron-confined-phonon interactions.

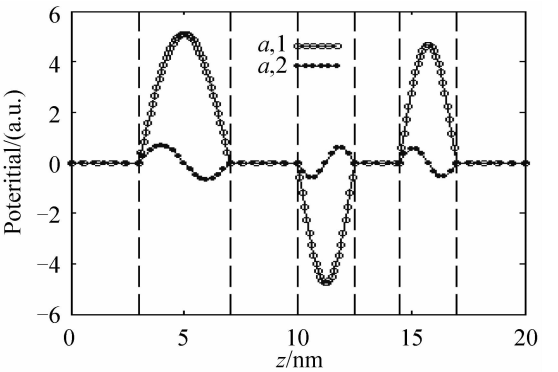

Fig. 5　The phonon potentials of modes a, 1 and a, 1 in C_{II} domain at $q=0.3$ nm^{-1}

3　Scattering rates in QCL

The electron-optical-phonon interactions play an important role in carrier scattering between both levels of the intersubband lasers. The scattering rate is derived from the Fermi's golden rule. We adopt the theoretical model of Lu to make the calculations[12-13], in which the the strong anisotropy of wurtzite is taken into accout. The scattering rates W_{31} and W_{21} between the lasing levels and the ground level in QCL are shown in Fig. 6. Here E_k is needed for the transition with subband separation smaller than phonon energy. we take $\triangle E_{21}=91$ meV, which is is close to the zone-center energy (90.8 meV) of GaN A_1(LO) mode. As for W_{21} induced by the confined modes, we can see the scattering rate of the C_I mode (at the left of dashed line) is smaller than that of the C_{II} mode (at the right of line), as should be this reason that the confinement of the C_{II} mode is much stronger in the wells. W_{21} induced by the interface modes reaches its maximum at $E_k=4.3$ meV, in

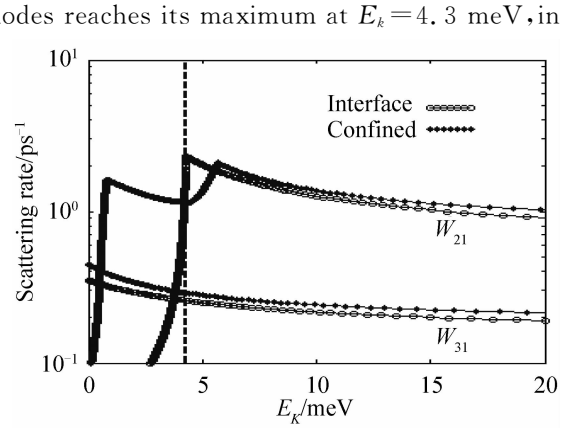

Fig. 6　The scattering rates W_{21} and W_{31} versus the initial in-plane electron energy E_k

which the sum of $\triangle E_{21}$ and E_k is just equal to the zone-center energy of AlGaN A_1(LO) phonon. For $\triangle E_{31}=119$ meV, W_{31} is far lower than W_{21}, owing to no resonance with the LO phonon, as is also advantaged for QCL to obtain population inversion between level 3 and 2. The scattering rate of the confined mode is comparable to that of the interface mode, and we think the strong effect of electron-confined-phonon interaction is attributed to the relatively wide wells in QCL.

Yu and Cao have calculated the scattering rates W_{31} and W_{21} induced by interface phonon in the GaAs-based cubic QCL[15], which are quantitatively smaller than, but the same order of magnitude as the scattering rates in the GaN-based wurtzite QCL. Sun has calculated the lifetimes τ_{31} and τ_{21} in AlGaN/GaN QCL[4], i. e., $W_{31}=0.37*10^{12}$ s^{-1}, and $W_{21}=4.2*10^{12}$ s^{-1}, which are calculated by using bulk GaN phonon modes. We find that the both scattering rates proposed by Sun almost accord with the counterpart induced by the interface or confined phonon in our paper.

4 Conclusion

We use the TMM model to investigate the interface and confined phonons in the AlGaN/GaN QCL. The interface modes exist in $[\omega_{\perp L,\mathrm{GaN}}, \omega_{zL,AlGaN}]$, meanwhile two groups of confined modes correspond to $[\omega_{zL,\mathrm{GaN}}, \omega_{\perp L,\mathrm{GaN}}]$ and $[\omega_{zL,\mathrm{AlGaN}}, \omega_{\perp \mathrm{L},\mathrm{AlGaN}}]$. The potentials of the interface phonons reach their maximum at the interfaces, and those of the confined modes are almost confined in the wells. Only the first three confined modes are considered to calculate the scattering rates, and we find the scattering rate induced by the confined mode is comparable to that induced by the interface mode. Furthermore we find it helpful to enhance the population inversion in QCL that $\triangle E_{21}$ must be palced in resonance with the LO phonon energy, meanwhile $\triangle E_{31}$ and $\triangle E_{32}$ must be kept away.

References

[1] GIANORDOLI S, SCHRENK W, STRASSER G, *et al*. Strained InGaAs/AlGaAs/GaAs-Quantum Cascade Lasers[J]. *Appl Phys Lett*, 2000, **76**(23): 3361-3363.

[2] STRASSER G, GIANORDOLI S, HVOZDARA L, *et al*. GaAs/AlGaAs superlattice quantum cascade lasers at $\lambda\approx13$ μm[J]. *Appl Phys Lett*, 1999, **75**(10): 1345-1347.

[3] ULRICH J, KREUTER J, SCHRENK W, *et al*. Long-wavelength (15 and 23 μm) GaAs/AlGaAs quantum-cascade lasers[J]. *Appl Phys Lett*, 2002, **80**(20): 3691-3693.

[4] SUN G, SOREF R A, KHURGIN J B. Active region design of a terahertz GaN/$Al_{0.15}Ga_{0.85}N$ quantum cascade laser[J]. *Superlattices and Microstructures*, 2005, **37**(2): 107-113.

[5] HUANG G S, LUA T C, YAO H H, *et al*. GaN/AlGaN active regions for terahertz quantum cascade lasers grown by low-pressure metal organic vapor deposition[J]. *J Cryst Grow*, 2007, **298**: 687-690.

[6] LI Chao, LI Xue, XU Jin-tong, *et al*. Tranmission spectra of GaN and AlGaN films[J]. *Acta Photonica Sinica*, 2009, **38**(9): 2294-2298.

[7] LI Xue, WEI Yan-feng, GONG Hai-mei, *et al*. Study on optical characteristics of wurtzite GaN[J]. *Acta Photonica Sinica*, 2007, **36**(2): 304-307.

[8] KOMIRENKO S M, KIM K W, STROSCIO M A, *et al*. Dispersion of polar optical phonons in wurtzite quantum wells [J]. *Phys Rev B*, 1999, **59**(7): 5013-5021.

[9] GLEIZE J, RENUCCI M A, FRANDON J, *et al*. Anisotropy effects on polar optical phonons in wurtzite GaN/AlN superlattices[J]. *Phys Rev B*, 1999, **60**(23): 15985-15990.

[10] KOMIRENKO S M, KIM K W, STROSCIO M A, *et al*. Optical phonons in wurtzite crystals and quantum wells[J]. *Phys Rev B*, 2000, **61**(3): 2034-2040.

[11] CHEN C, DUTTA M, STROSCIO M A. Confined and interface phonon modes in GaN/ZnO heterostructures[J]. *J Appl Phys*, 2004, **95**(5): 2540-2546.

[12] LU J T, CAO J C. Interface and confined optical-phonon modes in wurtzite multi-interface heterostructure[J]. *J Appl Phys*, 2005, **97**(3): 033502-033507.

[13] LU J T, CAO J C. Confined optical phonon modes and electron-phonon interactions in wurtzite ZnO/GaN quantum wells[J]. *Phys Rev B*, 2005, **71**(15): 155304-155308.

[14] YU S, KIM K W, STROSCIO M A, *et al*. Long-wavelength optical phonons in ternary nitride based crystals[J]. *Phys Rev B*, 1998, **58**(23): 15283-15287.

[15] YU B, CAO J C. Simulation of confined and interface phonons scattering in terahertz quantum cascade laser[J]. *Chin Phys Lett*, 2005, **22**(9): 2403-2406.

纤锌矿型量子级联激光器的界面与受限声子比较

陈贵楚[1]，范广涵[2]

(1 肇庆学院 物理系，广东 肇庆 526061)

(2 华南师范大学 光电子材料与技术研究所，广州 510631)

摘　要：利用传输矩阵方法对纤锌矿型量子级联激光器有源区的界面与受限声子进行了研究. 计算结果显示：在纵光学频域有一组界面声子与二组受限声子存在，而且最低频率的两个界面声子在一定条件下能转变为受限模式. 通过比较界面声子与受限声子的色散及声子势发现两者有很大不同，且计算电声散射速率可以发现由这两种声子引起的散射率是可比拟的.

关键词：AlGaN/GaN；量子级联激光器；界面；受限；散射率

CHEN Gui-chu　was born in 1973. Now he is pursuing his Ph. D. degree at South China Normal University, and his research interests focus on the material and physics of the optoelectronic device.

FAN Guang-han　was born in 1945. He is a professor and a Doctoral Supervisor, and his research interests focus on MOCVD epitaxy of the optoelectronic devices.